Bandwidth-Adaptive Single- and Double-Channel Silicon Photonic Contra-Directional Couplers

(Article begins on next page)

01 September 2025
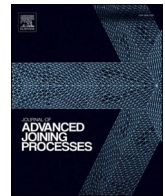
Effect of thermally expandable particle additives on the mechanical and reversibility performance of adhesive joints

Giulio Piazza [a], Matthew Burczyk [a], Marco Gerini-Romagnoli [a], Giovanni Belingardi [b], Sayed A. Nassar [a,*]

[a] Fastening and Joining Research Institute (FAJRI), Department of Mechanical Engineering, Oakland University, Rochester, MI, United States
[b] Politecnico di Torino, Turin, Italy

ABSTRACT

This paper provides an experimental investigation of the effect of Thermally Expandable Particle (TEP) adhesive additive on the mechanical and reversibility performance of epoxy-bonded load single lap joints (SLJs). Joint substrates are made of aluminum 6061 and woven carbon fiber reinforced plastic 0/90/0 substrates. TEP additive is used for modifying the structural epoxy adhesive used in this study. An electrically charged RF coil is placed around the joint bond area; generated electromagnetic field would heat the aluminum substrate which would in turn heat the modified adhesive. Very large volumetric expansion of the hollow spherical Thermally Expandable Particles (TEPs) would significantly reduce adhesive strength and lead to joint debonding under a minimal load of 100 N. Various weight concentrations of the TEP in the range of 5% to 25% with particulate size from 6 to 16 μm are used for investigating the effect on joint static and fatigue strength as well as the reversibility performance. Measured time to achieve full debonding of the joint (under charged RF coil), is used for assessing the reversibility performance.

Introduction

Fuel economy requirements, emissions regulations, environmental impact associated with the increasing use of multi-material design on the End-of-Life phase (EoL) and the push for energy independence are key factors driving the industry towards the increase of the vehicle efficiency. Environmental demands for reducing carbon emissions are driving the need to improve vehicle fuel economy, while increasing, on the other hand, the vehicle performance and passenger comfort (Modi et al., 2017). Over the last several decades, demands have significantly increased for weight reduction, because of fuel efficiency and energy saving considerations. On the other hand, however, increased demands for meeting stringent vehicle safety standards and emission regulations, have resulted in adding more components to the vehicle and that caused an increase of the overall vehicle weight (Soo, 2018; Zoepf, 2011), which increased the need to use multi/dissimilar materials to reduce vehicle weight. As a result, the need has increased significantly for reliable material joining process.

Joining dissimilar materials presents challenges because of the mismatch in mechanical, physical, and chemical properties of the components that are joined (Brandon and Kaplan, 1997). One of the main issues that occurs when joining dissimilar materials is galvanic corrosion. Designers need to make efforts to isolate the joint between conventional materials and Carbon Fiber Reinforced Plastic (CFRP), and the use of adhesive bonding as a joining technique offers a great advantage, avoiding direct contact between the two dissimilar components (Taub, 2006).

Adhesive joining is a strong candidate for particularly difficult material combinations such as metals to composites and/or polymers (Ebnesajjad and Landrock, 2014). Adhesives have a long list of advantages for mixed material applications such as their ability to join materials with dramatically different melting points while also sealing and separating dissimilar substrates, which in other cases would cause corrosion. Adhesive bonding also allows for a uniform load distribution and reduces stress concentration areas usually caused by mechanical fasteners and welding.

On the other hand, the choice of this joining technique will cause some drawback. Adhesives are difficult to manage, requiring special surface treatment, and can be characterized by slow curing time, not optimal for industrial process due to increased cycle time. Additionally,

adhesives are generally difficult to disassembly. A wide variety of applications are available in the literature, both scientific papers and industrial applications have demonstrated that this type of joining technology can lead to great performance while maintaining the efficiency in costs and timing.

Adhesive bonding research is recently going through some major changes. In the last years, studies have focused on the achievement of the reversibility of adhesively-bonded joints. Many studies have been conducted using different types of adhesive matrix, substrates (such as metallic, non-metallic, and composites) and additives combinations. Ciardiello (Ciardiello et al., 2017) studied the effect of particulate size of iron-based particles on mechanical properties of single lap joints and found that a Hot-Melt Adhesive (HMA) modified with the smallest iron particles showed no significant strength reduction. (Banea et al., 2015a, b) and (Veloso, 2015) studied the effect of the addition of different weight percentages of Thermally Expandable Particles (TEPs) in two different adhesive matrices, using metallic substrates. They found that the joint's mechanical performance would strongly depend on the TEPs concentration in the adhesive. Banea et al. (Banea et al., 2018a) studied the effect of moisture uptake on the behavior of a structural adhesive modified with TEPs. Due to the effect of aging, both the elastic modulus and tensile strength of the studied TEPs-modified adhesive were reduced, but after drying the tensile properties were recovered. Banea et al. (Banea et al., 2020) studied the effect of fatigue loading on single lap TEPs-modified adhesive joints and decrease in fatigue life was found for TEPs-modified adhesive joints in comparison to unmodified joints. Hutchinson et al. (Hutchinson et al., 2010) studied the effect of the addition of five different physical foaming agents and four different chemical foaming agents in three different automotive structural epoxy-based adhesives. One-time reversibility of a structural adhesive is possible, but each adhesive matrix will react in a unique way to the presence of additives.

In this paper, Thermally Expandable Particles (TEPs) are added to a structural adhesive in order to achieve the reversibility of an adhesive bonded multi-material Single Lap Joint (SLJ). The static and dynamic performance of these SLJs are tested to see the effect of the particles. Reversibility performance is evaluated by the debonding time of the joint and the temperature at debonding. Certain combinations of weight concentration of particles are subjected to corrosion cycling and tested for their static and reversibility performance.

Experimental procedure and test setup

Bonded Single Lap Joints composed of Aluminum and Carbon Fiber are tested in this work. One of the two substrates is made of Aluminum 6061-T6 with a thickness of $1/16''$ (1.6 mm), while the second one is made of woven carbon fiber (CFRP 0–90–0, aligned with the SLJ axes) in an epoxy matrix, with a thickness of $1/16''$ (1.6 mm). The selection of a woven reinforced carbon fiber is not casual. The substrates have to be able to respond to the induction heating caused by an electromagnetic field. Both substrates are pretreated. The bond area of aluminum substrates are scuffed with a wire drill brush, and subsequently cleaned with acetone. The carbon fiber substrates are manually scuffed with sandpaper to avoid fiber tear on the coupons and subsequently cleaned with acetone.

The adhesive used is Betamate 73,326/73,327 M, which is a two-part epoxy that is a commercially available structural adhesive. The lap shear strength of the properly mixed baseline adhesive is 11 MPa with aluminum substrates, and its bulk elastic modulus is 1100 MPa. The adhesive is modified with different weight percentages of Thermally Expandable Particles. The particles used are the Expancel 031DU40 (large) and 461DU40 (small) particles. For the 0461DU40 particles weight concentrations of 5%, 10%, and 20% are used, while for the 031DU40 particles weight concentrations of 5%, 10%, 15%, 20%, and 25% are used. Properties of the additive powder are shown in the Table 1. Depending on the size of the particles, the diameter can expand

Table 1
Thermally expandable particle characteristics.

Particle	Particulate Size (μm)	T_{start} (°C)	$T_{MaxExpansion}$ (°C)
031DU40	10 - 16	80 - 95	120 - 135
461DU40	6 - 9	100 - 106	143 - 150

from anywhere to 2–5 times the original diameter when the particles reach the required temperature resulting in a potential volume expansion of 8–125 times the original volume. A SEM image of the large particles (031DU40) inside the adhesive matrix before and after heating is shown in Fig. 1.

The particles and adhesive are mixed using an automated mixer (model DAC600FVZ) at a speed of 2100 rpm for 2 min and then again at 2100 rpm for an additional minute. After, the particles and adhesive are mixed in a bubble free vacuum mixer, first at 1000 rpm for 2 min, and then at 1775 rpm for 1.5 min. The joints follow an oven accelerated curing at 65 °C for four hours to avoid any expansion of the particles while curing.

The specimens are tested according to a slightly modified version of the ASTM Standards Test method for lap shear Adhesion for Fiber Reinforced Plastic bonding (D5968_01) (ASTM 2011). The main difference from the standard procedure is the bond line thickness that is reduced from 0.76 mm (0.03'') to 0.2 mm (0.079'') in order to use the most commonly used thickness in automotive applications. The specimens loading rate is 13 mm/min (0.5''/min). Tests are conducted using an MTS machine (Fig. 2). The substrates are 25.4 mm (1'') wide and 101.6 mm (4in) long, the overlap area between the substrates is 25.4 mm x 25.4 mm (1'' x 1'') or 6.45 cm² (1 in²).

Experimental fatigue data is collected using an 810 MTS testing system. The test samples are cycled to failure at one mean stress level and three different alternating stresses. The fatigue tests are performed on weight concentrations of 5%, 10%, and 20%. Screening tests have been performed using three different levels of mean stress equal to 30% 35% and 40% of the baseline static Load Transfer Capacity (LTC). Three different amplitude levels are used to generate S-N curves where the stress amplitude is plotted against the number of cycles to failure, on a log-log scale. The mean stress level that has been chosen for the study continuation is equal to the 35% of the maximum LTC. This value is used for all the different adhesive/additive combinations.

Statistical methods are available to assist in this analysis of experimental data and recommendations for their use are found in the literature (ASTM 1998; BSI 1976). Two statistical methods are used for analyzing fatigue test data: namely the 95% confidence interval and 95% prediction interval. The first interval defines the limits inside which a given proportion (95%) of the coefficients of the regression line (which generates the S-N line) fall. The second bound, instead, establish the limits between which a given proportion (95%) of all the data lie. The two bands are used to compare different distributions; if the bands of two different set of data are overlapping, the behaviors of the two compared samples are considered statistically equivalent. Those bands are determined respectively using the following relations:

$$\log N_{P\%}^{\pm} = (\log A + m\log S) \pm t\hat{\sigma}\sqrt{\frac{1}{n} + \frac{(\log S - \overline{\log S})^2}{\sum_{i=1}^{n}(\log S_i - \overline{\log S})^2}} \qquad (1)$$

$$\log N_{P\%}^{\pm} = (\log A + m\log S) \pm t\hat{\sigma}\sqrt{1 + \frac{1}{n} + \frac{(\log S - \overline{\log S})^2}{\sum_{i=1}^{n}(\log S_i - \overline{\log S})^2}} \qquad (2)$$

where: log(A) and m are the coefficients of the regression line through the n data points (log S_i, log N_i); log(S) is the mean of the n values of log S_i. t is the Student's coefficient for the appropriate confidence level; $\hat{\sigma}^2$ is the best estimate of the variance of the data about the regression line,
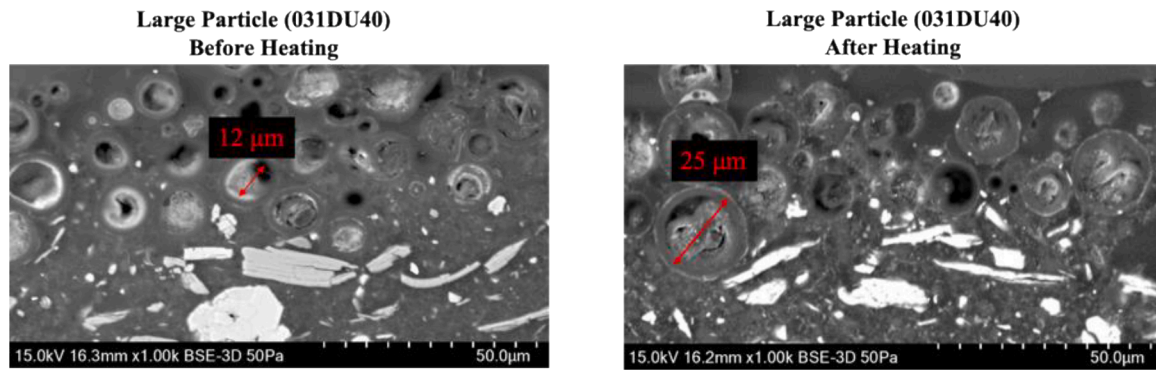
Fig. 1. SEM images of adhesive cross section 031DU40 particles before and after heating.
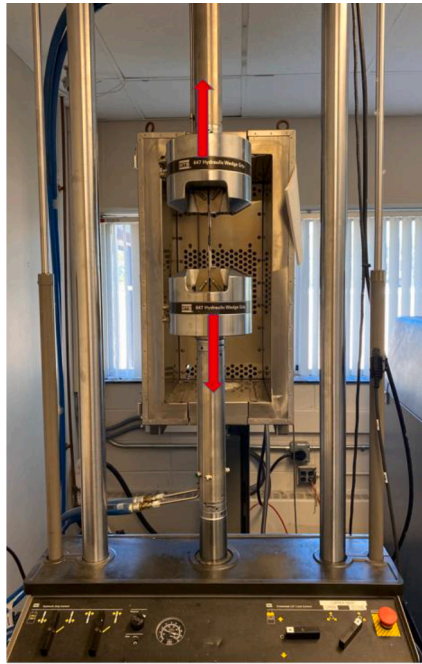

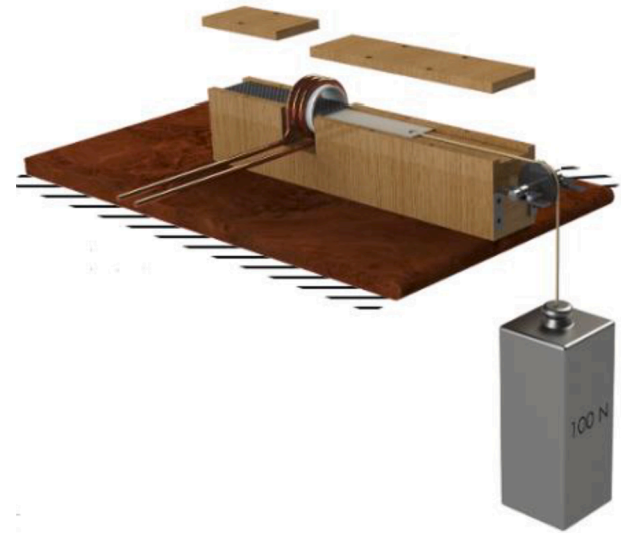**Fig. 2.** MTS 810 material test system.

Fig. 3. Schematic of debonding fixture.

which is equal to the sum of squared residuals divided by the number of degrees of freedom f; f is equal to $n - 2$ in the case where the two coefficients of the regression line have both been estimated from the data.

The debonding tests are performed using an RDO HFI 3.0 kW RF heating system. The frequency range is 135–400 KHz and it can be tuned to suit a variety of applications. The joints are placed inside the helical RF coil attached to the RDO machine. The coil induces an electric current in the substrate at the bond-line. Once the adhesive reaches a certain temperature, the added particles expand in volume, thus aiding in the debonding of the joint. For the tests, the frequency is set in the range of 330–338 Hz and the power is set at 210 W. A constant 100 N load is applied to the joint while it is heated inside the coil. Holes are drilled on the end of both substrates in order to achieve the test set up as shown by Fig. 3. The carbon fiber end of the joint is placed on the pin while a rope is tied on the aluminum substrate. The 100 N load is applied by a rope/pulley system. During the tests, the time to achieve debonding and the temperature of the substrate are recorded. Debonding is considered successful if the substrates of the joint separate in 10 min or less. Any samples that are not able to separate, are maintained at room temperature for 24 h, and a lap shear test is conducted to determine the residual strength of the joint.

The corrosion cycling of the joints with 5%, 15% and 25% particle

enrichment (031DU40) is performed to explore how the enriched adhesive responds to different levels of temperature and humidity. The cyclic corrosion test that is performed is the GMW 14,872 test (General Motors Corporation 2006). It is an accelerated corrosion test method to evaluate assemblies and components. The corrosion cycling is done using a CCT-NC-20 Cyclic Corrosion Chamber. The first of the three different stages is an ambient stage at 25 °C and 45% relative humidity, with intermittent sprays of the salt solution. The second stage is a humid stage at 49 °C and 100% relative humidity, with a one-hour ramp. The final stage is the dry off stage at 60 °C, with less than 30% relative humidity, and a three-hour ramp. The corrosion cycling continuously runs and each stage is 8 h. The complex salt spray solution that is used is 0.9% sodium chloride (NaCl) by mass, 0.1% calcium chloride (CaCl$_2$) by mass, 0.075% sodium bicarbonate (NaHCO$_3$) by mass, and 98.925% Water (H$_2$O) by mass.

Discussion of the results

This section provides experimental data analysis on the static, fatigue, corrosion, and reversibility performance of Aluminum/CFRP single lap joints with modified structural epoxy adhesive, for various additive concentrations and particulate size.

Static joint strength data is shown in Fig. 4, for various Expancel additive concentrations, with a relatively larger particulate size (031DU40) and a smaller particulate size (461DU20). The minimum sample size is 3 for each combination. More significant reductions in
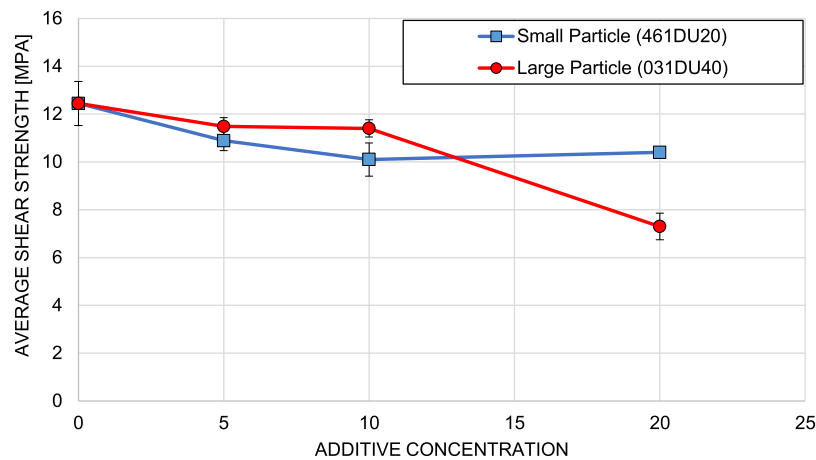
Fig. 4. Lap shear strength variation betamate 73,326/73,327 M for different additive concentrations.

static lap shear strength are observed for joints enriched with the smaller particulate size (461DU20), when compared to the larger particles (031DU40), for the 5wt% and 10wt% concentrations: joints modified with larger particulate experienced a 7.5% (5wt%) and 8.7% (10wt%) strength decrease from the baseline value, while the LTC of the samples enriched with smaller particles was reduced by 12.7% (5wt%) and 19% (10wt%). The opposite behavior is observed for 20wt% enriched samples: larger particle size (031DU40) samples experience a more severe reduction in LTC (41%) when compared to the smaller particulate size (461DU20) samples (19%).

Both particles cause a decrease in adhesive strength when added to the adhesive matrix. Joints modified with larger particulate (031DU40) experience a gradual LTC decrease with increasing concentration, while the addition of smaller particles (461DU20) to the adhesive causes an initial decrease in strength for concentrations up to 10 wt.%; no additional strength loss is observed increasing the concentration from 10% wt. to 20wt% (Fig. 4).

For a given enrichment level, joints modified with smaller additive particles (461DU20) contain a larger number of particles than test samples modified with larger diameter (031DU40) additives. The adhesive's mechanical behavior is almost perfectly elastic, and the higher amount of localized stress concentration induced by the larger number of smaller particles can be used to explain the initial drop in joint performance, at lower concentrations. At higher weight concentrations, the particles occupy a significant portion of the adhesive layer, and their mechanical behavior contributes to the joint's performance. The strength of the additive microspheres is inversely proportional to their diameter, thereby explaining the significant drop in LTC experienced by joints modified with larger particulate.

The effect of the GMW 14,872 corrosion cycling on the static strength of adhesive joints with 5, 15, and 25% concentration of the large particles (031DU40) is shown in Fig. 5, with 1σ error bars. Under the applied conditions corrosion does not have a statistically significant impact on the average lap shear strength for the baseline adhesive or for adhesive modified with concentrations of 5% wt. and 25% wt. For the 15% wt. samples, a decrease in strength is shown after 29 and 42 days of corrosion cycling.

The failure mode for all of the enriched samples is cohesive. The 5% wt. enriched samples remains fully cohesive without any significant variation in the fracture surface, when compared to the baseline adhesive. When the concentration is increased to 10%, the failure mechanism is still cohesive, but starts to show some changes in the area where the peel stress is at its peak: a step forms in the fracture surface for all concentrations higher than 10%. The variation of the failure fracture surface and its location appear to be caused by two main factors, the first is the difference in flexural rigidity between the carbon fiber and the aluminum substrates, the second is the reduction in strength of the bulk adhesive. The variation of the peel stress along the adhesive thickness is studied. The stress gradient through the adhesive thickness is numerically evaluated at "Point A" and "Point B" (Fig. 6).

The peel stress gradient at the two sides of the structure is plotted in Fig. 6 and it is highest at the end of the aluminum substrate (Point B). The variation in the fracture surface is observed in correspondence to Point B because the variation of peel stress along the adhesive thickness and its absolute value are much more accentuated in that area when compared to the opposite side. In that section it is possible to observe that the fracture surface shifts from the middle of the bondline towards the aluminum adherend.
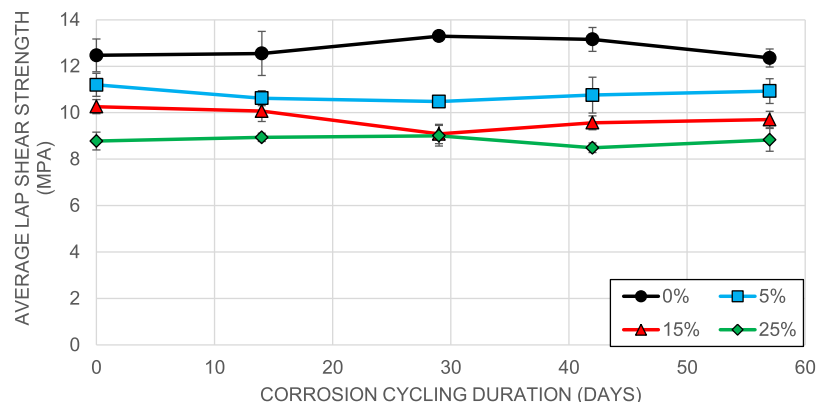

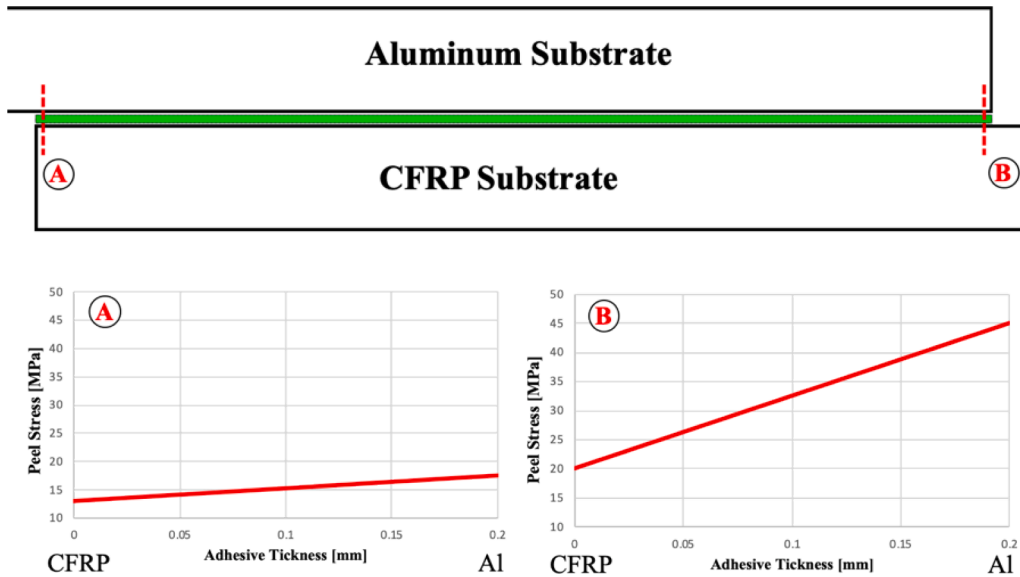**Fig. 5.** Average lap shear strength vs corrosion cycling duration (large particles 031DU40).

Fig. 6. Peel stress gradient along the adhesive thickness: a) carbon fiber side b) aluminum side.

Fatigue test results

This section includes test data and analysis for the effect of concentration and micro-particle size of the additive on the fatigue performance of the joints. Fatigue data is generated under a set mean load that is fixed at 35% of the respective static strength (LTC) of each test joint combination. Figs. 7-10 show the normalized fatigue strength; normalization is with respect joint static strength (LTC). The selected stress amplitude for all concentrations is shown in Table 2 below.

For all concentrations the absolute fatigue strength is significantly reduced by the presence of additives within the adhesive matrix. The results show that increasing the concentration also decreases the absolute fatigue strength. In order to investigate the significance of this data, the fatigue data is normalized with respect to the LTC of each enrichment level. The normalized data allows to infer whether or not the fatigue failure mechanism is affected by the presence of the additives. The normalized fatigue results are shown in Figs. 7 and 8, and 95% prediction intervals are shown on the S-N curves in Figs. 9 and 10.

Figs. 7 and 8 show the data points for the fatigue performance of the small particles and large particles respectively at 5, 10, and 20% enrichment levels compared to the baseline adhesive. For clarity, only the baseline S-N curves are drawn. The normalized figures show a clear overlap of both the data points and S-N curves for all enrichment levels and the baseline adhesive. This overlap shows that difference between

Table 2
List of alternating stress levels for fatigue testing.

Additive Concentration (Wt.)	Particulate size (Commercial ID)	Alternating Stress (% of LTC)
5%	Smaller (461DU20)	25, 20, 15
	Larger (031DU40)	20, 15, 10
10%	Smaller (461DU20)	24, 18, 12
	Larger (031DU40)	20, 15, 10
20%	Smaller (461DU20)	20, 15, 10
	Larger (031DU40)	20, 15, 10

the normalized fatigue strength of the baseline adhesive and the enriched adhesive is not significant.

Figs. 9 and 10 show the S-N curves and the 95% prediction interval for the fatigue performance of the small and large particle respectively, for enriched samples and baseline adhesive. Results are presented for the sample 20% enrichment level to prevent overcrowding. Like in Figs. 7 and 8, there is a clear overlap of both the S-N curves and the 95% prediction intervals for the baseline and 20% enriched adhesive. These graphs, which are normalized with respect to their own LTC, further demonstrate that the fatigue failure mechanism of the adhesive joints is not altered by the addition of TEPs.

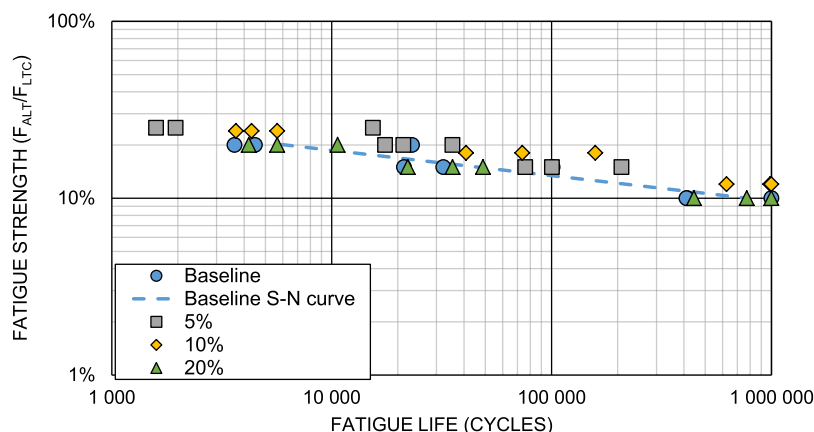The decrease in absolute fatigue strength is due to a reduction in the

Fig. 7. Fatigue data for enriched adhesive vs baseline adhesive (small particle 461DU20, normalized).
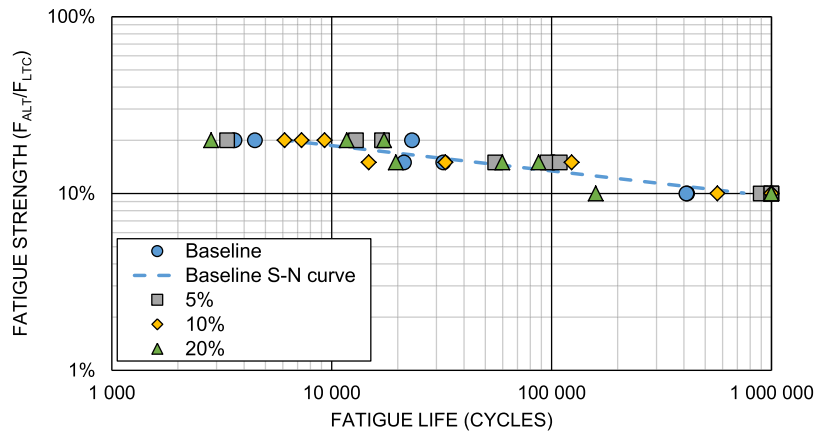
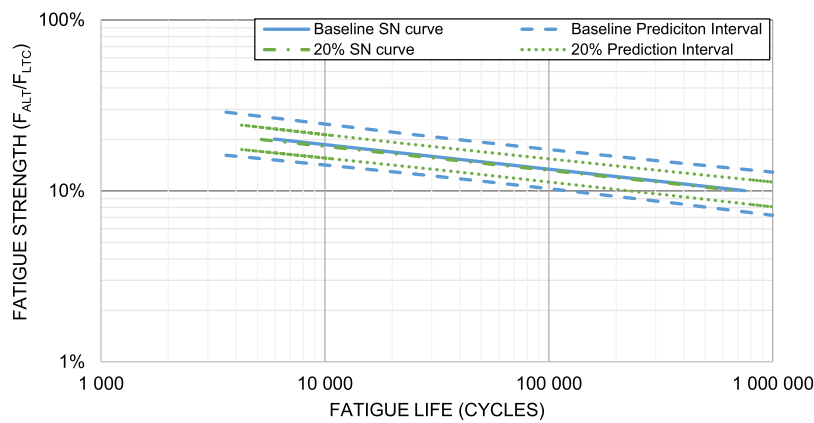**Fig. 8.** Fatigue data for enriched adhesive vs baseline adhesive (large particle 031DU40, normalized).

Fig. 9. Fatigue data for enriched adhesive vs baseline adhesive 95% prediction interval (small particle 461DU20, normalized).
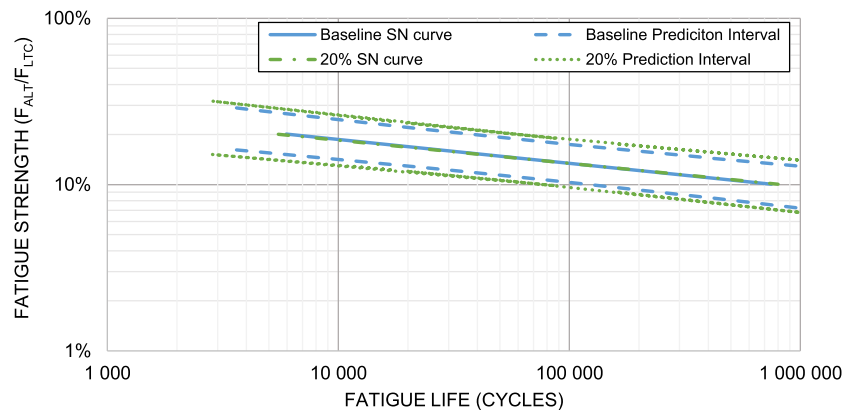

Fig. 10. Fatigue data for enriched adhesive vs baseline adhesive 95% prediction interval (large particle 031DU40, normalized).

LTC. The addition of TEPs in the bondline cause a decrease in resistant cross-sectional area, reducing the static lap shear strength of the adhesive SLJs. However, the expandable microsphere do not appear to cause significant increases in stress concentration in the adhesive layer, which would lead to more severe crack initiation and propagation. This would be shown by a significant difference in the normalized fatigue performance figures.

For all of the debonding tests a time limit of 10 min is set and any joints that reach this limit are considered to have survived the test. The system is fine tuned to allow for the workpiece to follow a desired temperature path. An initial ramp (210 W) is then followed by a steady

state condition (150 W). The substrate temperature profile is shown in Fig. 11.

The temperature profile for the enriched adhesive is shown in Fig. 11. For concentrations of 10% wt. and 20wt% the debonding temperature of the joints is 114 °C and 94 °C for the large particles, and 101 °C and 99 °C for the small particles. The reason that the debonding temperature does not reach temperatures as high as the baseline or 5% concentration adhesive is that successful joint separation is achieved for concentrations of 10wt% and 20wt%. Increasing the particle concentration increases the mechanical separation of the joint. The debonding temperature of the substrate is dependent on the time it takes for the
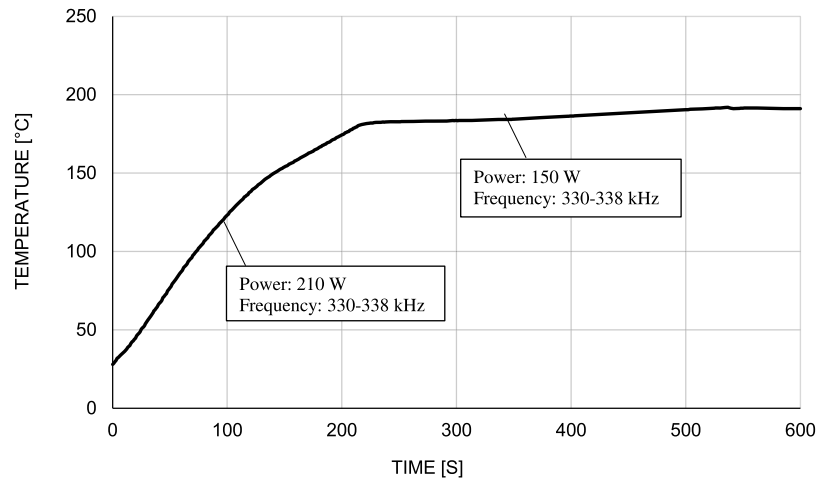
Fig. 11. Substrate temperature profile large particles (031DU40).

joint to separate, which is why there is variation on the debonding temperature for different concentrations and particle sizes. The longer the joint takes to separate, the higher the debonding temperature.

The dependence between weight concentration and time to debond for different particles is shown in Fig. 12. The test data shows that additive concentration does not significantly affect the debonding time for smaller particle size additive. The debonding time of the adhesive enriched with the larger particle size (031DU40) is highly dependent on the particle concentration. For both particle sizes, a 5% concentration of particles is not enough to allow for joint separation in the debonding test as all test samples did not debond in 10 min.

The effects of corrosion on debonding time are shown in Fig. 13. For the 25% wt. of larger particles, the applied corrosion conditions has no effect on the debonding time. Corrosion has a significant effect on the debonding performance of joints with 15% wt. of large particles. After 42 days of corrosion cycling, only one of the test specimens is able to successfully debond, and after 57 days, none of the test specimens are able to debond. The corrosion cycling likely allows for moisture to penetrate the adhesive. If moisture is able to penetrate the thermoplastic shell of the particles, then some particles will not be able to expand, causing the number of expandable particles aiding in joint separation to decrease during the debonding testing. The 25% wt. samples likely contain a large enough concentration of particles to overcome the effects of the corrosion on the particles.

Residual strength of the specimens that are not able to achieve debonding is shown in Figs. 14 and 15. All baseline adhesive samples and 5% wt. samples (both particulate sizes) survive the debonding test. Some of the corrosion cycled 15% wt. enriched samples survive as well. The modified adhesive joints experience drastic load bearing capacity

reduction with less than 50% of the initial strength left after that the samples were heated. The applied corrosion conditions do not have a significant impact on the residual strength as shown in Fig. 14. The volumetric expansion of the particles is responsible for the static strength reduction.

Conclusions

This study shows that chosen Thermally Expandable Particle (TEP) additive to modify Epoxy structural adhesive caused reduction of the static strength of adhesively bonded aluminum/composite joints. The absolute fatigue strength of the adhesive decreased with addition of the particles, but this was not significant as the fatigue strength normalized with respect to each enrichment level's LTC showed no significant difference in fatigue performance. The addition of TEP additives to structural adhesive allows successful adhesive bond reversibility for some of the chosen levels of additive concentration. Bond reversibility was possible for concentrations larger than 5% wt.; namely, by using 10%, 15%, 20%, or 25% concentration of the additive in the epoxy adhesive. Both the time and temperature to debond were decreased for additive concentrations of 10% and 20%. Aside from the decreased initial level of joint strength caused by the modified adhesive, the subsequent corrosion cycling of test samples did not cause significant change in the static strength. However, corrosion cycling showed significant effect on the reversibility performance of joints with 15% wt. concentration of the additive to the Epoxy adhesive.
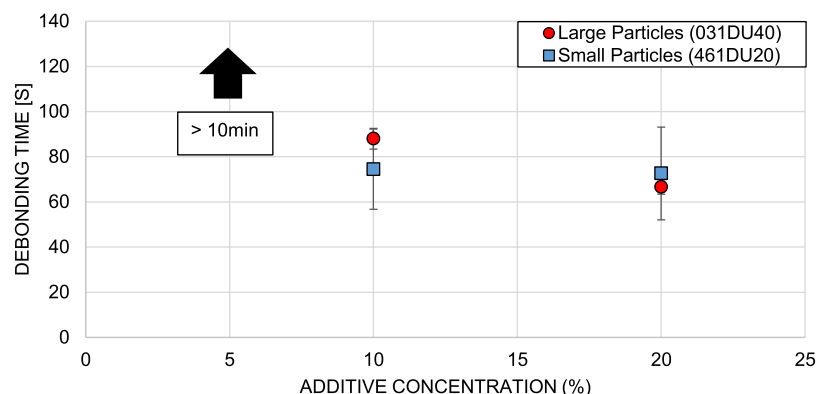

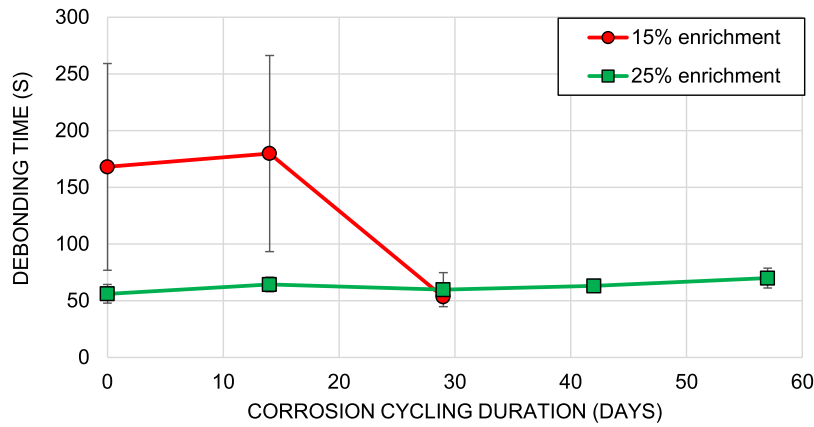**Fig. 12.** Time to debond vs additive concentration.

Fig. 13. Effect of corrosion cycling on debonding time (large particles 031DU40).
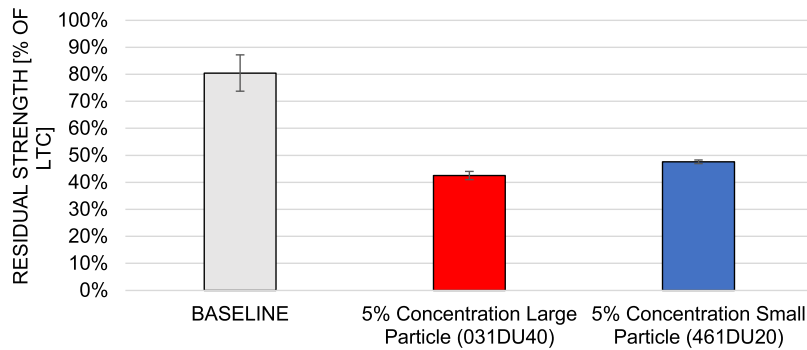

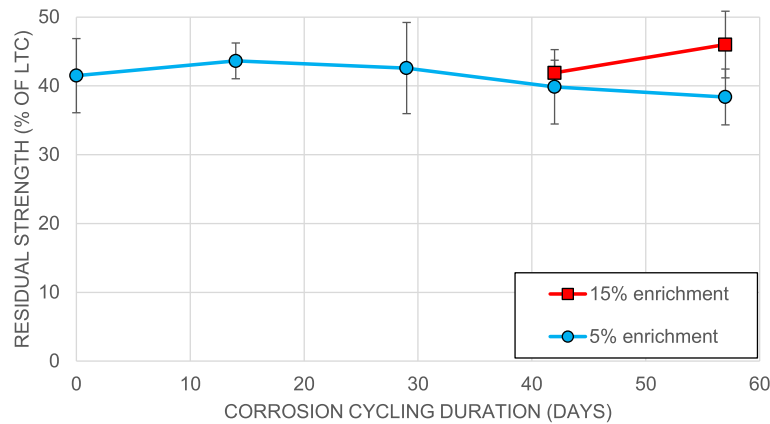**Fig. 14.** Residual strength after heating.

Fig. 15. Effect of corrosion cycling on residual strength after heating.

Declaration of Competing Interest

No conflict of interest. 'Copyrights Permission from ASME has been requested'.

References

ASTM, 1998: "ASTM Practice for statistical analysis of linear or linearized stress-life (S-N) and strain-life (ε-N) fatigue data', ASTM E-739-91, West Conshohocken, PA.

ASTM, 2011: "Annual Book of ASTM standards, section fifteen, general products, chemical, specialties, and end use products", ASTM Volume 15.06., Adhesives.

Banea, M., Da Silva, L., Carbas, R., Cavalcanti, D., De Souza, L., 2020. The effect of environment and fatigue loading on the behaviour of TEPs-modified adhesives. J. Adhes. 96, 1–4. https://doi.org/10.1080/00218464.2019.1680546, 423-436.

Banea, M., da Silva, L., Carbas, R., 2015a. Debonding on command of Adhesive joints for the automotive industry. Int. J. Adhesion Adhesive 59, 14–20.

Banea, M., da Silva, L., Carbas, R., Barbosa, A., Viana, G., 2018a. Effect of the water on the behavior of adhesives modified with thermally expandable particles. Int. J. Adhesion Adhesives 91, 823–840.

Banea, M., da Silva, L., Carbas, R., Campilho, R., 2015b. Structural adhesives modified with thermally expandable particles. J. Adhes. 91, 10–11. https://doi.org/10.1080/00218464.2014.985785, 823-840.

Banea, M., Rosioara, M., Carbas, R., da, Silva, L., 2018b. Multi material adhesive joints for automotive industry. Comp. Part B 150, 71–77.

Brandon, D., Kaplan, W., 1997. "Joining Processes, An Introduction", ISBN 0-471-96488-3. Wiley-VCH, New York, Hoboken, NJ.

BSI, 1976: "Guide to statistical interpretation of data", BS 2864, London.

Ciardiello, R., Martorana, B., Lambertini, V., Brunella, V., 2017. Iron-based revesible adhesives: effect of particle size on mechanical properties. Inst. Mech. Eng. 232 (8), 1446–1455. https://doi.org/10.1177/0954406217736552. IMechE.

Ebnesajjad, S., Landrock, A., 2014. Adhesives Technology Handbook, 3rd ed. William Andrew, Elsevier, London, UK.

General Motors Corporation, November 2006, "GMW Test Procedure Materials: GMW14872", general motors worldwide engineering standards.

Hutchinson, A., Winfield, P., McCurdy, R., 2010. Automotive material sustainability through reversible adhesives. Adv. Eng. Mater. 12 (7), 646–652.

Modi, S., Stevens, M., Chess, M., 2017. Mixed Material Joining Advancements and Challenges. Center for Automotive Research (CAR), Ann Arbor, MI.

Soo, V., 2018. Life Cycle Impact of Different Joining decision on Vehicle Recycling. The Australian National University, Camberra, Australia.

Taub, A., 2006. Technology trends and challenges in the 21st century. Automotive Mater., MRS BULLETIN Volume 31, 336–343.

Veloso, R., 2015. Debonding on Command of Adhesive Joints for the Automotive Industry. MS Thesis. Istituto Politecnico de Viseu, Viseu, Portugal.

Zoepf, S., 2011. Automotive Features: Mass Impact and Deployment Characterization. Massachusetts Institute of Technology, Cambridge, MA.